# Path Accommodation Methods for the Bidirectional Ring with Optical Compression TDM

**Kazuhiro Gokyu** [*], **Ken-ichi Baba** [†], **and Masayuki Murata**[*]

## Abstract

In this paper, we propose path accommodation methods for bidirectional rings based on an optical compression TDM (OCTDM) technology. We first derive a theoretical lower bound on the number of slots and frames, which is necessary to allocate all paths among nodes. The relationships between the lower bound and such parameters as the compression rate and the numbers of transmitters/receivers are then discussed. Three path accommodation algorithms are next proposed to achieve the lower bound as close as possible. Through numerical examples, we show that each of three algorithms has best parameter regions achieving the best results. Our recommendation is therefore that three algorithms are all performed, then the best one is chosen. Finally, we analyze the packet delay time for given number of slots and frames that our algorithms decided. Numerical examples show the characteristics of packet delays in various conditions.

## 1 Introduction

According to a rapid growth of a user population and multimedia applications on the Internet, traffic volume has been dramatically increasing on backbone networks. In the metropolitan area, the backbone ring is promising to build MAN (Metropolitan Area Network), which inter-connects LANs (Local Area Networks) of companies, laboratories, ISPs (Internet Service Providers), and so on. An optical-electric exchange was conventionally used in routers or switches for the access from LAN to MAN. However, an all-optical access without the optical-electric exchange is now essential to realize high-speed MANs (see, e.g., [1, 2]).

A packet-switched ring with all-optical access can be realized by optical wavelength-division multiplexing (WDM) or optical time-division multiplexing (OTDM) techniques. In WDM, high speed transmission over 10 Gbps on a single wavelength can be obtained, but a limited number of wavelengths inhibits many-to-many communication among nodes at the same time. In the OTDM system, on the other hand, it is easier to control communication facilities than in the WDM system, and a recent development of an optical pulse compression/expansion technology [3, 4] makes it more attractive, by which the backbone network with one to two magnitudes of larger capacities can be provided. In [3], for example, the backbone ring with an optical pulse compression/expansion technology, called OCTDM (Optical Compression TDM), is now being produced experimentally, where LANs with 622 Mbps are interconnected by the backbone OCTDM ring with one to tens of Gbps. In their proposal, when the optical node of the OCTDM ring receives the packet from LAN, bit intervals are shortened to fit the transmission rate of the backbone ring. The packet is then lengthened at the destination node. See Section 2 for more details.

In OCTDM, we need some routing policy on how each slot within the frame is used by nodes. In conventional TDM, one possible and natural way to accommodate the traffic on the ring is to assign the slot as follows; the number $N$ of nodes on the ring is numbered from 0 to $N-1$. Then, $i$th slot within the frame (consisting of $N$ slots) is assigned to $i$th source node, so that $i$th source node always transmits the packet on $i$th slot within destination address. In this scheme, the destination node may receive at most $N$ packets during the frame time. In OCTDM, however, the number of slots that the node can access within the frame is limited by the number of costly receivers [5]. Since the number of transmitters is also limited, another method that $i$th slot is reserved for $i$th destination node is not adequate for the OCTDM ring as well. Accordingly, we need a path accommodation method suitable to the OCTDM ring in this paper by taking account of those facts. Here, by "path", we mean the assigned slot(s) for a pair of source/-destination nodes.

In the path accommodation method considered in this paper, paths between every source/destination

[*] K. Gokyu, and M. Murata are with the Department of Informatics and Mathematical Science, Graduate School of Engineering Science, Osaka University, Toyonaka, Osaka 560–8531, Japan (e-mail:{gokyuu, murata}@ics.es.osaka-u.ac.jp).

[†] K. Baba is with the Computation Center, Osaka University, Ibaraki, Osaka 567–0047, Japan (e-mail:baba@center.osaka-u.ac.jp).

pair are determined a priori for given traffic load matrix. In the receiver-oriented approach in which $i$th slot is reserved for $i$th destination node described above, some contention resolution mechanism among the source nodes is necessary. It must introduce an unacceptable overhead. Another approach also exists. A medium access control method such as a token passing method (DQDB or FDDI) might be applied to the OCTDM ring. However, the delay of control signals including the propagation delays between nodes much degrades performance of the OCTDM ring with very high-speed capacity. We thus do not consider such approaches in the current paper.

As a related work, the path design method in the WDM ring is reported in [6], where the cost effective design method is proposed for accommodating the *wavelength path* for every node pair. In their method, the number of wavelengths is a limited factor. In their companion paper [7], the time needed to accommodate all paths with the given number of wavelengths is also obtained. They consider the fixed packet length, and therefore, the time is slotted in the WDM system. Thus, their system becomes similar to our OCTDM ring. Actually, we will borrow their idea in one of path accommodation methods that we will examine in this paper. However, we extend the their method in [7] to make it possible to treat the heterogeneous traffic load for node pairs, while the original method assumed the homogeneous traffic load. Also, the theoretical lower bound presented in Section 3 is an extension of the approach described in [7].

The rest of the paper is organized as follows. In Section 2, we briefly describe the OCTDM ring structure and our model. In Section 3, we develop the lower bound on the number of frames necessary to accommodate all paths for given parameters (the numbers of transmitters/receivers and the compression rate), and investigate the relationship between the lower bound and system parameters. In Section 4, three path accommodation algorithms are considered. The effectiveness of those algorithms is then compared based on the theoretical lower bounds shown in Section 3. In Section 5, we analytically obtain the packet delay time, and show influences of several parameters on the packet delay. Conclusions and future works are summarized in Section 6.

## 2 The Structure of OCTDM Ring Networks

### 2.1 Optical Pulse Compression/Expansion Technique

An optical pulse compression/expansion technology is promising to realize the very high-speed backbone ring [5]. When the packet is put on the optical line, a bit interval is compressed by using the fiber delay loop (Figure 1). Since the compression rate with one loop is limited, high compression rate can be achieved by using several steps if it cannot be realized at a time. A semiconductor optical amplifier (SOA) and the switch (SW) are inserted on the loop to compensate the loss on the fiber delay loop. Then, the packet is transmitted onto the ring. When the packet is received from the optical line to LAN, bit expansion is performed as a reverse procedure of bit compression. More details of the optical pulse compression technique are described in [8, 9, 10].

### 2.2 Access Method to Rings

We consider a bidirectional ring consisting of two unidirectional, working fiber links; one clockwise and the other counter-clockwise.

Each ring of two directions is slotted. The packet arriving at the node is divided into *mini-packet*s at the source node. The mini-packet with additional header is put in the slot assigned for the source/destination pair. The assignment method of slots is our objective of the current paper, which will be described in the following sections. The mini-packet is transmitted to the ring after it is optically compressed with $K$ times, and each frame consists of $K$ slots. That is, the compression rate $K$ is identical to the number of slots within the frame.

There are $N$ nodes on the ring. The nodes are numbered clockwise from $0$ to $N-1$. Nodes $i$ and $i+1$ is connected by link $i$. See Figure 2. The node structure is shown in Figure 3. We assume that node $i$ has the number $T_i$ of transmitters and $R_i$ of receivers. Each transmitter can send only one mini-packet once per each frame in either direction. Each receiver can receive only one mini-packet per each frame as well. That is, transmitters and receivers are shared in both directions. The number of mini-packets that each node can transmit (receive) in the frame is thus limited by the number of transmitters (receivers). Noting that each node cannot receive more packets than the number of the receivers in one frame, an optical memory is unnecessary in the above configuration. It is attractive since the optical memory technology is still not mature for packet buffering.

Since the compression rate $K$ is usually much smaller than the number of nodes $N$ (which is a natural assumption from the current and probably future technologies), slots for all source/destination node pairs cannot be put within the frame. We will call a *super-frame* for the number of frames which can accommodate all paths (i.e., the number of slots for every pair of source/destination nodes). In Section 3, we will derive a theoretical lower bound for the length of the super-frame. Then, in Section 4, we

will propose three path accommodation algorithms to assign slots to all nodes for given traffic load matrix. The effectiveness of those path accommodation algorithms is then investigated by comparing the theoretical lower bound.

## 3 Derivation of Theoretical Lower Bounds

### 3.1 Introduction of Notations

Let $\mathcal{T} = \{T_0, T_1, \cdots, T_{N-1}\}$ and $\mathcal{R} = \{R_0, R_1, \cdots, R_{N-1}\}$ be sets of the number of transceivers and receivers, respectively.

The path from source node $i$ to destination node $(i+s)$ is represented by $(i, s)$, where $s$ is the clockwise distance in hops between two nodes. A counter-clockwise distance is represented by the negative number. However, to make representation simple in the following analyses, we will allow to use some $k$ $(\geq N)$ in representing the node number. In that case, $k$ should be read as $mod(k, N)$. Similarly, the negative values of the node number and the node distance are also allowed. Namely, $k \leftarrow N - mod(|k|, N)$ if $k < 0$. For example, in the case of $N = 64$, node $68$ means node $4$, and node $-7$ does node $57$. The node distance $-13$ shows the distance $51$ if we consider the distance clockwise.

In this and next sections, we assume that the traffic load is expressed in integer values, i.e., the required number of slots for path $(i, s)$ takes an integer value $c^{(i,s)}$. A $N$ by $N$ matrix $C = \{c^{(i,s)}\}$ is given as the traffic load matrix. Hereafter, we implicitly assume that the total sum of the traffic load does not exceed the backbone ring capacity, so that it is always possible to accommodate all of paths.

Since we consider the bidirectional ring, there is a freedom to choose the path for two nodes clockwise or counter-clockwise. We assume using the shorter path. When the number of nodes is even, there are two shortest paths between node $i$ and $(i + \frac{N}{2})$. In that case, we use the path for $(i, \frac{N}{2})$ as follows;

- When $0 \leq i \leq \lfloor \frac{N}{4} \rfloor - 1$, or $\frac{N}{2} \leq i \leq \lfloor \frac{N}{4} \rfloor + \frac{N}{2} - 1$, the path is set up clockwise.
- Otherwise, use the path counter-clockwise.

### 3.2 Derivation of Lower Bounds

In this subsection, we derive the lower bounds of the super-frame length for given $N$ (the number of nodes), $\mathcal{T}$ (a set of the number of transmitters), $\mathcal{R}$ (a set of the number of receivers), $K$ (a compression rate of OCTDM), and $C$ (a traffic load matrix). We define it as $LB(N, \mathcal{T}, \mathcal{R}, K, C)$. Note that the theoretical lower bound in WDM rings was studied in [7] under the conditions (1) that the numbers of transmitters and receivers provided by all nodes are identical, and (2) that the traffic load is uniform. We extend the method presented in [7] for our OCTDM ring under the non-uniform traffic load.

**(A) The case where $\mathcal{T}$ and $\mathcal{R}$ are infinite, and $K$ is finite**

We first consider the case where the compression rate $K$ is finite, but the numbers of transmitters/receivers at every node are infinite. We denote the total number of clockwise (counter-clockwise) paths on the link $i$ by ${n_R}^{(i)}$ ${n_L}^{(i)}$, which can be determined from traffic load matrix, $C$, as:

$$ {n_R}^{(i)} = \sum_{j=(i+1)+\lceil \frac{N}{2} \rceil}^{i+N} \sum_{s=(i+N+1)-j}^{\lfloor \frac{N}{2} \rfloor} c^{(j,s)} \cdot r_d^{(j,s)}, \quad (1) $$

$$ {n_L}^{(i)} = \sum_{j=i+1}^{i+\lfloor \frac{N}{2} \rfloor} \sum_{s=\lceil \frac{N}{2} \rceil}^{i+N-j} c^{(j,s)} \cdot l_d^{(j,s)}, \quad (2) $$

where $r_d(i, s) = 1$ if path $(i, s)$ is set up clockwise; $r_d^{(i,s)} = 0$ if counter-clockwise. Similarly, $l_d^{(i,s)} = 0$ if path $(i, s)$ is set up clockwise; $l_d(i, s) = 1$ if counter-clockwise.

Since each frame has $K$ slots, the number $K$ of paths can be set up in each frame on link $i$ in either of two directions. It then requires $\lceil \frac{{n_R}^{(i)}}{K} \rceil$ frames to allocate all of clockwise paths on link $i$. It is also true for counter-clockwise paths. The theoretical lower bound of the super-frame length, $LB(N, \infty, \infty, K, C)$ is thus given as:

$$ LB(N, \infty, \infty, K, C) = \max_{0 \leq i \leq N-1} (\lceil \frac{{n_R}^{(i)}}{K} \rceil, \lceil \frac{{n_L}^{(i)}}{K} \rceil). \quad (3) $$

**(B) The case where $K$ is infinite, and $\mathcal{T}$ and $\mathcal{R}$ are finite**

The total number of paths from sender node $i$ to the other receiver nodes is given by ${s_p}^{(i)} = \sum_{s=1}^{N-1} c^{(i,s)}$. Similarly, the total number of paths from sender nodes except node $i$ to the receiver node $i$ is given by ${r_p}^{(i)} = \sum_{k=0}^{N-1} c^{(k,i-k)}$. The infinite compression rate ($K = \infty$) means that the number of slots in each frame is infinite. The number of paths allocated for node $i$ is bounded by the numbers of transmitters, ($T_i$) and receivers ($R_i$). That is, $LB(N, \mathcal{T}, \infty, \infty, C)$ and $LB(N, \infty, \mathcal{R}, \infty, C)$ are derived as;

$$ LB(N, \mathcal{T}, \infty, \infty, C) = \max_{0 \leq i \leq N-1} (\lceil \frac{{s_p}^{(i)}}{T_i} \rceil), \quad (4) $$

$$ LB(N, \infty, \mathcal{R}, \infty, C) = \max_{0 \leq i \leq N-1} (\lceil \frac{{r_p}^{(i)}}{R_i} \rceil). \quad (5) $$

From two cases (A) and (B) above, we can obtain $LB(N, \mathcal{T}, \mathcal{R}, K, C)$ using Eqs. (3)–(5) as follows:

$$ LB(N, \mathcal{T}, \mathcal{R}, K, C) = \max_{0 \leq i \leq N-1} (\lceil \frac{n_R^{(i)}}{K} \rceil, \lceil \frac{n_L^{(i)}}{K} \rceil, \lceil \frac{s_p^{(i)}}{T_i} \rceil, \lceil \frac{r_p^{(i)}}{R_i} \rceil). \quad (6) $$

From Eq. (6), we can observe that the length of the super-frame can become smaller if terms in Eq. (6) are uniformly distributed for given numbers of transmitters/receivers and the compression rate. Then we have the ring with high throughput. We will give quantitative examples in the following subsection.

### 3.3 Numerical Results and Discussions

In this subsection, we investigate the relationship between the lower bounds of the super-frame length and several system parameters including the number of nodes, the numbers of transmitters and receivers, and the compression rate. In the OCTDM ring, the increase of the number of transceivers leads to the shorter super-frame, which results in decreasing the lower bound. However, it needs the large optical buffer (realized by the optical lines) [11]. Even when the number of transceivers can be provided, the super-frame length is not decreased if the compression rate $K$ is small. It is because the compression rate poses a limit on the number of slots assigned for each node. Then, the throughput cannot be improved.

We first consider the uniform traffic load condition. The traffic matrix $C_1$ has elements with all 1's, i.e., $c^{(i,s)} = 1$ except elements, $c^{(i,0)} = 0$. The number of nodes is set to be 64. See Figure 4(a). Every node on the ring has the identical number $T$ of transmitters, i.e., $\mathcal{T} = \{T, T, \cdots, T\}$. Similarly, the number of receivers of all nodes is also identically set to be $R$. Figure 5 plots the lower bounds for traffic matrix $C_1$. From the figure, we can observe that as the numbers of transmitters and receivers are increased, the lower bound shows a gradual decrease, and finally becomes constant. For instance, in the case of the compression rate of 20 (i.e., $K = 20$), the lower bound becomes constant when $T = R \geq 3$. That is, the lower bound is not limited by the numbers of transmitters/-receivers but the compression rate in this parameter region. If $T = R = 1$ (which is a current technological level), then the compression rate of $K \geq 9$ does not help improve the lower bound (and the total throughput of the ring).

We next investigate the case of the non-uniform traffic demand. As shown in Figure 4(b), the traffic demand to the receiver node 63 is increased to 2 in the traffic matrix $C_2$. (Note that the traffic matrices $C_3$ and $C_4$ in Figures 4(c) and 4(d) will be used in the next section.) Other demands are same as in the traffic matrix $C_1$ (Figure 4(a)). The lower bounds for $C_2$ are plotted in Figure 6. In obtaining this figure, the number of transmitters/receivers at every node is identically set. Figure 6 shows the substantial increase of the lower bounds when compared with Figure 5. For example, the length of the super-frame is increased from 32 to 64 for $T = R = 2$ and $K \geq 16$. It means that the maximum throughput of the ring is halved with a slightly increased traffic to the receiver node 63.

If we add the receiver at node 63, however, the length of the super-frame can be again decreased. The results are presented in Figure 7. As shown in the figure, the number of receivers at node 63 is increased by one, while the numbers of transmitters/-receivers at other nodes remain unchanged. Namely, the resource balance is very important to attain the short super-frame in the OCTDM ring.

In this section, we have considered the theoretical lower bounds given by Eq. (6). However, Eq. (6) only provides the bound, and the path accommodation algorithm is necessary to actually allocate the path(s) (i.e., slot(s)) to all source/destination pairs of nodes and to determine the length of the super-frame, which will be described in the next section.

## 4 Path Accommodation Algorithms and Comparisons

In this section, we first describe three path accommodation algorithms in Section 4.1. It is difficult to obtain an optimal allocation since examination on all combinations is necessary to find it. Three accommodation algorithms presented in the below are all heuristic. The degree of an optimality of those algorithms is investigated by comparing with the lower bounds developed by the previous section, which will be presented in Section 4.2.

### 4.1 Path Accommodation Algorithms

In the algorithm A1, the path with the largest distance is chosen first to allocate the path. The traffic loads on links and nodes are taken into account in the algorithm A2. The algorithm A3 is an extension of the one described in [7], where the paths are determined according to quadrilateral paths accommodation. In what follows, we will describe those algorithms in turn.

#### 4.1.1 Algorithm A1: The longer path is assigned first.

We first describe the algorithm A1, which attempts to assign slots to the longest path. It is simple that it does not consider the traffic load condition on every link and node. However, as will be demonstrated in the next subsection, the algorithm A1 outperforms other two algorithms in some parameter sets.

The algorithm A1 first finds the source/destination pairs requesting the path with longest distance (i.e., $s = \lfloor \frac{N}{2} \rfloor$). For those paths, the slot is assigned from source node 0 to $(N-1)$ if the source/destination pair requests such a path. The transmitter for the source node and the receiver for the destination node are also examined. In doing so, the path is examined clockwise and counter-clockwise alternately. Then, next longest paths with distance $s = \lfloor \frac{N}{2} \rfloor - 1$ are assigned. All paths are examined until paths with distance 1 are assigned slots.

See Appendix A for its procedure. The procedure `CEP(`$i, s$`)` (Check and Establish a Path) in the algorithm first checks to see if transmitters, receivers, and slots are available to set the path $(i, s)$ when $c^{(i,s)} \geq 1$. If it is true, path $(i, s)$ is actually set. Then, $c^{(i,s)}$ is decremented by one.

#### 4.1.2 Algorithm A2: The path with the highest traffic load is set first.

In the second algorithm A2, the path using most links, transmitters, and receivers is first set. More specifically, the algorithm works as follows. Let us introduce a $N \times N$ traffic weight matrix $C_W = \{w^{(i,s)}\}$. It shows the sum of the weighting factors on the link, transmitter, and receiver along path $(i, s)$, the element of which is determined as follows:

- If path $(i, s)$ is set clockwise because it has a smaller distance, then
$$w^{(i,s)} = \lceil \frac{\sum_{k=i}^{i+s-1} {n_R}^{(k)}}{K} \rceil + \lceil \frac{{s_p}^{(i)}}{T_i} \rceil + \lceil \frac{{r_p}^{(i+s)}}{R_{i+s}} \rceil . \quad (7)$$
- If path $(i, s)$ is set counter-clockwise, then
$$w^{(i,s)} = \lceil \frac{\sum_{k=i+s}^{i+N-1} {n_L}^{(k)}}{K} \rceil + \lceil \frac{{s_p}^{(i)}}{T_i} \rceil + \lceil \frac{{r_p}^{(i+s)}}{R_{i+s}} \rceil . \quad (8)$$
- $w^{(i,s)} = 0$ if $c^{(i,s)} = 0$.

The setup is first tried for the path with maximum element of $C_W$. During the algorithm execution, the traffic weight matrix $C_W$ should reflect the changes of the traffic load matrix $C$ every frame such that the paths having been already set up are excluded.

See Appendix B for the algorithm A2. The variables `max_cw_i` and `max_cw_s` are the row and column numbers of the maximal element of $C_W$, respectively. The function `CP(`$i, s$`)` (Check a Path) checks utilizations of transceivers, receivers and slots if path $(i, s)$ can be set up when $c^{(i,s)} \geq 1$. It returns 'true' if those resources can be used; otherwise it returns 'false'. The procedure `EP(`$i, s$`)` (Establish a Path) sets path $(i, s)$ and then execute $c^{(i,s)} = c^{(i,s)} - 1$ if $c^{(i,s)} \geq 1$. The procedure `CALC(`$a_1, a_2, \cdots$`)` calculates the parameters $a_1, a_2, \cdots$ from $C$ at a time.

#### 4.1.3 Algorithm A3: an extended CADS

The algorithm A3 is a modified and extended version of the CADS algorithm, which was originally proposed for the WDM ring [7]. Note that in [7], the CADS algorithm is applied for the case where the number $N$ of nodes is even and the CATS algorithm is for $N$ odd, but those algorithms are essentially same. Therefore, we only consider the CADS algorithm here. We first show a part of the CADS algorithm in Appendix C where paths are set up clockwise. In the CADS algorithm, two paths between two nodes, which are located on the diagonal of rings are chosen at the same time. Those are then set up along the same direction. It is performed in Step 1. Then, four paths corresponding to edges of the rectangle are set up at the same time along the same direction in Steps 2 and 3.

The CADS algorithm can only be applied to the case where the traffic load is uniform. It chooses a combination of the long-distance and short-distance paths to construct the rectangle. Without loosing the basic philosophy of the algorithm, we extend it to be applicable to any traffic load matrix. It is the algorithm A3, which is shown in Appendix D. When the traffic load is non-uniform, every paths are not always set up at the same time. Thus, each path should be set up independently. Note that the algorithm A3 works exactly same as the CADS algorithm when the traffic load is uniform.

### 4.2 Comparisons of Three Path Accommodation Algorithms

In this subsection, we compare three algorithms A1, A2 and A3 presented in the previous subsection. The number of nodes, $N$, is fixed at 64. The numbers of transmitters and receivers per node are assumed to be identical; i.e., $T = R$. For the traffic load matrix, we will consider $C_3$ (Figure 4(c)) and $C_4$ (Figure 4(d)) in addition to previously used $C_1$ and $C_2$. Characteristics of those matrices are summarized as follows.

- $C_1$: a uniform traffic load.
- $C_2$: all paths except the ones with receiver node 63 are uniform. The load of paths from any source node to receiver node 63 is two times larger than that of others.
- $C_3$: similarly to $C_2$, all paths except the ones with receiver node 63 are uniform. The load of any node to receiver node 63 is three times larger than that of others. That is, non-uniformity of the traffic load of $C_3$ is higher than $C_2$.
- $C_4$: all paths except the ones with receiver nodes 33 and 63 are uniform. The load of paths from any node to receiver nodes 33, and 63 is three times larger than that of others.

Figure 8 compares the theoretical lower bounds on the length of the super-frame (labelled by 'LB') derived in Section 3 and the results of three algorithms, dependent on the compression rate $K$. Figures 8(a) through 8(d) are for the traffic matrices $C_1$, $C_2$, $C_3$ and $C_4$, respectively. In these figures, the number of frames achieving the smallest value among three algorithms is shown with bold-face. From Figure 8(a), we can observe that the Algorithm A3 is the best choice for the uniform matrix $C_1$. However, for matrices $C_2$, $C_3$ and $C_4$, the algorithm A2 also exhibits good results as algorithm A3. It is especially true for small values of $T$ and $R$. It is a good feature of algorithm A2 if we consider the current technological level of optical transceivers. We also note that algorithm A1 becomes best in rather extreme cases in-

cluding the cases of $T = R = 8$ and $K = 1$ for matrix $C_4$.

A more close look at the results is presented in Figures 9 through 12 using matrices $C_1$, $C_2$, $C_3$ and $C_4$, respectively. In each of those figures, results of the Algorithm A1, A2 and A3 are plotted. In obtaining all figures, the numbers of transmitters and receivers ($T$ and $R$) are identically set and varied from 1 to 12, and the compression rate $K$ are from 1 to 64. The numbers achieving the theoretical lower bound are represented by '■', and the best result among three algorithms is shown by '□'. As mentioned in the above, the algorithm A3 is appropriate for matrix $C_1$, excluding the case of $T = R = 1$. On the other hand, best results are often provided by the Algorithm A2 for matrices $C_2$, $C_3$, and $C_4$. It means that the algorithm A2 considering traffic loads is effective as we expect.

In summary, the algorithm A3 provides better results than others especially when the traffic load is uniform. If the traffic load is non-uniform, however, the algorithm A2 also works well and often provides better results than the algorithm A3. The effectiveness of the algorithm A1 is limited, but it appears in cases such as the number of transceivers is small, which is a realistic assumption in the current technology. That is, we could not find the best algorithm working best in all parameter regions. Thus, our conclusion and recommendation in this section are that all three algorithms should be performed to find the best solution.

## 5 Analysis of Packet Delay Times

In Sections 3 and 4, we have considered that the traffic load is given in unit of slot times. Then, we considered the path accommodation algorithms which determine the super-frame length to accommodate all traffic. In doing so, we have assumed that the total traffic load does not exceed the backbone ring capacity. In this section, we again assume it to derive the delay time of packets arriving at the node.

We first assume the uniform traffic load. By assuming it, only one slot is assigned within the super-frame for given source/destination pair. When the packet consisting of the multiple mini-packets arrives, each mini-packet is transmitted using the slot. That is, after the packet with $n$ mini-packets reaches the head of the queue at the source node, it takes the super-frame length (in time) multiplied by $n$ to transmit all mini-packets.

In the following analysis, we will assume that packets arrive at the source node according to the Poisson distribution. The number of mini-packets contained in the packet follows the general distribution. Then, we can utilize the result of the M/G/1 queueing system to derive the packet delay time. We note here that the packets are first buffered at the LAN side, and therefore, we do not need optical buffer to store the packets at the source node.

In what follows, we will consider the source/destination pair of the path $(i, s)$ to derive the packet delay. The uniform traffic load is first treated in Section 5.1. The result presented in Section 5.2 provides the approximate packet delay for the non-uniform traffic load.

### 5.1 Analysis of Packet Delay Times for the Uniform Traffic Load Case

By letting the LAN capacity be $B_L$ [bps], and the unidirectional ring capacity $B_R$ [bps], we have the relation, $B_R = K \cdot B_L$. One slot time denoted by $t$ [s] is given by

$$t = \frac{(S_h + S_p) \cdot 8}{B_R}, \tag{9}$$

where $S_h$ [byte] and $S_p$ [byte] are the header and payload sizes of the mini-packet. The propagation delay between nodes $i$ and $(i + s)$ is denoted by $W_p^{(i,s)}$ [s]. Further, the number of frames in the super-frame is represented by $r$, which has been determined by our path accommodation algorithms in the previous section. Then, the number of slots contained in the super-frame, $D$, is given by $K \cdot r$ where $K$ is a compression rate of the optical ring.

We assume that at source node $i$, packets arrive according to a Poisson distribution with rate $\lambda^{(i,s)}$ destined for node $(i + s)$. Hereafter, we will derive the mean packet delay for this stream. The packet length in bytes has a general distribution with probability function $f$, and we represent its mean by $P_B$ [byte]. The traffic load (in bps) for path $(i, s)$ is then given by

$$B_f^{(i,s)} = \frac{\lambda^{(i,s)} \cdot P_B \cdot 8}{t}. \tag{10}$$

Further, we introduce the random variable $P_m$, representing the number of mini-packets in the packet. Its probability function, $g(n)$ $(n = 1, 2, \ldots)$, is given by

$$g(n) = \text{Prob}[P_m = n] = \sum_{x=S_p(n-1)+1}^{S_p \cdot n} f(x). \tag{11}$$

Our objective is to derive the packet delay time $W^{(i,s)}$ [s] on path $(i, s)$, which consists of four components;

$$W^{(i,s)} = \left( \frac{D}{2} + W_q^{(i,s)} + (E[T_F] - (D-1)) \right) \cdot t + W_p^{(i,s)}. \tag{12}$$

In what follows, we will consider each term of the right hand side of the above equation. The fourth term, $W_p^{(i,s)}$, is the propagation delay from source node $i$ to destination node $(i + s)$. The first term in braces is necessary because we consider the random arrival of packets, and the packet should wait the half

of the super-frame in average so that the first mini-packet can be put on the slot assigned to that path.

We next examine the third term in braces. The random variable $T_F$ [slots] in the term shows the mean time to transmit all mini-packets contained in the packet from the time when the designated packet reaches the head of the queue. Since it needs the number $E[P_m]$ of super-frames, the following equation holds;

$$E[T_F] = D \cdot E[P_m]. \tag{13}$$

The subtraction of $D-1$ from $E[T_F]$ is necessary since we consider the time interval until the last mini-packet is put onto the ring in this term.

The second term of the right hand side in Eq. (12), $W_q^{(i,s)}$, corresponds to the queueing time at the source node buffer until the packet reaches the head of the queue. By applying the Pollaczek-Khinchin formula, it can be obtained by

$$W_q^{(i,s)} = \frac{\lambda^{(i,s)} E[T_F^2]}{2(1-\lambda^{(i,s)} E[T_F])}, \tag{14}$$

where $E[T_F^2]$ is given by $D^2 E[{P_m}^2]$.

By rewriting Eq. (12), we finally have

$$W^{(i,s)} = \left[\frac{\lambda^{(i,s)} D^2 E[{P_m}^2]}{2(1-\lambda^{(i,s)} D E[P_m])} + D\left(E[P_m] - \frac{1}{2}\right) + 1\right] \cdot t + W_p^{(i,s)}. \tag{15}$$

### 5.2 Extensions to the Case of Non-Uniform Traffic Load

In the case of non-uniform traffic load, two or more slots may be assigned within a single super-frame for the source/destination pair. The positions of assigned slots depend on the path accommodation algorithm, and the intervals of slots may be irregular. Those make it impossible to derive the packet transmission time in a generic form as in the previous subsection.

Here, we introduce the assumption that assigned slots are uniformly distributed within the super-frame. More specifically, the chance to transmit the mini-packet destined for destination node $(i+s)$ visits its source node $i$ every $D/c^{(i,s)}$ slots. Note that $D$ and $c^{(i,s)}$ mean the number of slots of the super-frame and the number of slots assigned to path $(i,s)$ during the super-frame, respectively.

Then, the mean packet delay for the case of non-uniform traffic load can be derived by modifying Eq. (15) as

$$W^{(i,s)} \approx \left[\frac{\lambda^{(i,s)} (D/c^{(i,s)})^2 E[{P_m}^2]}{2(1-\lambda^{(i,s)} (D/c^{(i,s)}) E[P_m])} + \frac{D}{c^{(i,s)}}\left(E[P_m] - \frac{1}{2}\right) + 1\right] \cdot t + W_p^{(i,s)} \tag{16}$$

### 5.3 Numerical Examples and Discussions

Noticing that our main purpose of this section is to investigate the effect of several system parameters on the packet delay, we simply assume that the distribution of the packet size, $f(x)$, follows the geometric function, i.e.,

$$f(x) = (1-1/P_B)^{x-1} \cdot 1/P_B. \tag{17}$$

In the following numerical examples, we will use the following values; the mean packet size $P_B$ is set to be 500 [byte], the header size of the mini-packet $S_h$ is 2 [byte], the LAN capacity, $B_L$, is fixed at 622 [Mbps], and the total length of the optical ring is 500 [Km]. For other parameters, we will use nine parameter sets shown in Table 1, which will be explained later in presenting figures.

We first investigate the effects of the compression rate, $K$, and the number of frames within the super-frame, $r$. For this, we use the parameter sets $A$, $B$ and $C$ shown in Table 1. For the super-frame length, we use the theoretical lower bound obtained in Section 3 to exclude the effect of the optimality level of the path accommodation method. The effect of the selection of the path accommodation method will be investigated in the below. While the parameter sets A ($K=8$, $r=64$) and B ($K=16$, $r=32$) give a same length of the super-frame ($D=512$), Figure 13 clearly shows that the larger compression rate in the parameter set B leads to the smaller delay. Then, the maximum throughput becomes much larger. However, the larger compression rate does not always attain improved performance. It is illustrated by the parameter set C in which the compression rate of $K=32$, twice of the one in the parameter set B, is used. The results of the parameter sets B and C are very close. That is, the number of frames $r$ has a great impact on performance in this parameter region.

An example of the effect of path accommodation methods is shown by using parameter sets D, E and F in Table 1). By applying the Algorithms A1, A2 and A3, we obtained 43, 40 and 32 as the number of frames in those parameter sets. Figure 14 clearly shows that the number of frames much affects the mean packet delay time.

The effect of the mini-packet size is finally presented in Figure 15. Here, we set the mini-packet size, $S_i$, to be 53, 256 and 530 [byte] while the mean packet length remains unchanged. The different mini-packet sizes are considered in the parameter sets G, H and I of Table 1. The differences observed in Figure 15 are much affected by the mean and distribution of the packet length in the current case. Namely, we can observe that padding necessary for the last mini-packet cannot be ignored in obtaining high performance when the slot length is fixed

as in the current case of the OCTDM ring. We need a further research work to determine the appropriate slot length by taking account of the actual packet size distribution.

## 6 Concluding Remarks and Future Works

In this paper, we have proposed and evaluated the path accommodation methods for the bidirectional OCTDM rings, which are expected as the new generation all-optical networks.

We have first derived the theoretical lower bound for the length of the super-frame, in which all paths among nodes are perfectly allocated. The relationships between the lower bound and such parameters as compression rate, transmitters and receivers are then investigated. Three path accommodation algorithms are proposed next to treat the non-uniform traffic load. Through numerical examples, we have shown that the result obtained by our proposed algorithms is close to the lower bound. The mean packet delay time has also been analyzed.

As future works, the reliability issue for the OCTDM rings should be addressed, which is an important feature of optical networks. Also, the optical compression TDM/WDM where the optical compression is applied to each of wavelengths in WDM must be an interesting research topic.

## References


[1] *Proceeding of the SPIE Conference on All-Optical Networking 1999: Architecture, Control, and Management Issues*, Sept. 1999.

[2] Special issue on "WDM Fiber Optic Communications", *IEEE Communications Magazine*, vol. 36, no. 12, Dec. 1998.

[3] A. Hasegawa and H. Toda, "A feasible all optical soliton based inter-LAN link using time division multiplexing," *IEICE Transactions on Communications*, vol. E81-B, pp. 1681–1686, Aug. 1998.

[4] N. S. Patel, K. L. Hall, and K. A. Rauschenbach, "Optical rate conversion for high-speed TDM networks," *IEEE Photonics Technology Letters*, vol. 9, no. 9, pp. 1277–1279, Sept. 1997.

[5] B. Y. Yu, P. Toliver, R. J. Runser, K. L. Deng, D. Zhou, I. Glesk, and P. R. Prucnal, "Packet-switched optical networks," *IEEE Micro*, vol. 18, no. 1, pp. 28–38, Jan-Feb 1998.

[6] X. Zhang and C. Qiao, "On optimal scheduling and cost effective design in WDM rings," *IEEE/LEOS Broadband Optical Networks*, Paper TuB3, Aug. 1996.

[7] X. Zhang and C. Qiao, "On scheduling all-to-all connections and cost-effective designs in WDM rings," *IEEE/ACM Transactions on Networking*, vol. 7, no. 3, pp. 435–445, June 1999.

[8] K. L. Deng, K. I. Kang, I. Glesk, P. R. Prucnal, and S. Shin, "Optical packet compressor for ultra-fast packet-switched optical networks," *Electronics Letters*, vol. 33, no. 14, pp. 1237–1239, July 1997.

[9] H. Toda, F. Nakada, M. Suzuki, and A. Hasegawa, "An optical packet compressor using a fiber loop for a feasible all optical TDM network," *25th European Conference on Optical Communication (ECOC'99)*, vol. Tu C3.7, 1999.

[10] A. Hasegawa and H. Toda, "An optical packet compressor for a feasible all optical inter-LAN TDM network," *Broadband Access and Technology, European Conference on Networks and Optical Communications (NOC'99)*, pp. 233–238, 1999.

[11] K. L. Hall and K. A. Rauschenbach, "All-optical buffering of 40-gb/s data packets," *IEEE Photonics Technology Letters*, vol. 10, no. 3, pp. 442–444, Mar. 1998.

## Appendix A: Algorithm A1

01: $the\_super\text{-}frame\_length = 1$
02: while( every path cannot be set up ){
03: if( a path cannot be set up at all )
04: $the\_super\text{-}frame\_length++$
05: for( $s = \lfloor \frac{N}{2} \rfloor; s \geq 1; s--$ )
06: for( $i = 0; i \leq N-1; i++$ )
07: CEP( $i, s$ )
08: CEP( $i, N-s$ )
09: }
10: Decision of $the\_super\text{-}frame\_length$

## Appendix B: Algorithm A2

01: $the\_super\text{-}frame\_length = 1$
02: while( every path cannot be set up ){
03: CALC($n_R, n_L, s_p, r_p, C_W$)
04: while( a path can be set up ){
05: CALC($max\_cw\_i, max\_cw\_s$)
06: if(CP($max\_cw\_i, max\_cw\_s$)){
07: EP($max\_cw\_i, max\_cw\_s$)
08: }
09: else {
10: $w^{(max\_cw\_i, max\_cw\_s)} = 0$
11: }
12: }
13: $the\_super\text{-}frame\_length++$
14: }
15: Decision of $the\_super\text{-}frame\_length$

## Appendix C: CADS Algorithm ($N$ is even)

**Step 1:**
for $s = \frac{N}{2}$ (a special case)
for $i = 0, 1, \cdots, \frac{N}{4} - 1$
Two paths in the following
are set up at a time if possible.
$(i, \frac{N}{2}), (\frac{N}{2} + i, \frac{N}{2})$
**Step 2:**
for $s = \frac{N}{4}$ (a special case)
for $i = 0, 1, \cdots, \frac{N}{4} - 1$
Four paths in the following
are set up at a time if possible.
$(i, \frac{N}{4}), (\frac{N}{4} + i, \frac{N}{4}),$
$(\frac{N}{2} + i, \frac{N}{4}), (\frac{3N}{4} + i, \frac{N}{4})$
**Step 3:**
for $s = 1, 2, \cdots, \frac{N-2}{4}$ (general case)
for $i = 0, 1, \cdots, \frac{N}{2} - 1$
Four paths in the following
are set up at a time if possible.
$(i, s), (i + s, \frac{N}{2} - s),$
$(\frac{N}{2} + i, s), (\frac{N}{2} + i + s, \frac{N}{2} - s)$

## Appendix D: Algorithm A3

01: $the\_super\text{-}frame\_length = 1$
02: while( every path cannot be set up ){
03: if( a path cannot be set up at all )
04: $the\_super\text{-}frame\_length++$
05: for($i = 0\ i \leq \frac{N}{4} - 1\ i++$){ **(Step 1)**
06: CEP($i$, $\frac{N}{2}$)
07: CEP($i + \frac{N}{2}$, $\frac{N}{2}$)
08: }
09: for($i = 0; i \leq \frac{N}{4} - 1; i++$){ **(Step 2)**
10: //clockwise
11: CEP($i$, $\frac{N}{4}$)
12: CEP($i + \frac{N}{4}$, $\frac{N}{4}$)
13: CEP($i + \frac{N}{2}$, $\frac{N}{4}$)
14: CEP($i + \frac{3N}{4}$, $\frac{N}{4}$)
15: //counter-clockwise
16: CEP($i$, $\frac{3N}{4}$)
17: CEP($i + \frac{3N}{4}$, $\frac{3N}{4}$)
18: CEP($i + \frac{6N}{4}$, $\frac{3N}{4}$)
19: CEP($i + \frac{9N}{4}$, $\frac{3N}{4}$)
20: }
21: for($s = 1; s \leq \frac{N-2}{4}; s++$){ **(Step 3)**
22: for($i = 0; i \leq \frac{N}{2} - 1; i++$){
23: //clockwise
24: CEP($i, s$)
25: CEP($i + s$, $\frac{N}{2} - s$)
26: CEP($i + \frac{N}{2}, s$)
27: CEP($i + \frac{N}{2} + s$, $\frac{N}{2} - s$)
28: //counter-clockwise
29: CEP($i, N - s$)
30: CEP($i + N - s, N - (\frac{N}{2} - s)$)
31: CEP($i + \frac{3N}{2}, N - s$)
32: CEP($i + \frac{5N}{2} - s, N - (\frac{N}{2} - s)$)
33: }
34: }
35: }//while
36: Decision of $the\_super\text{-}frame\_length$

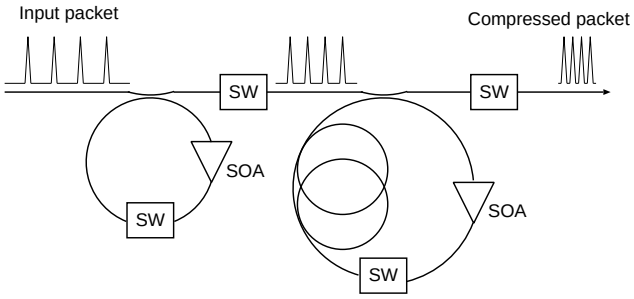


Figure 1: Optical packet compressor

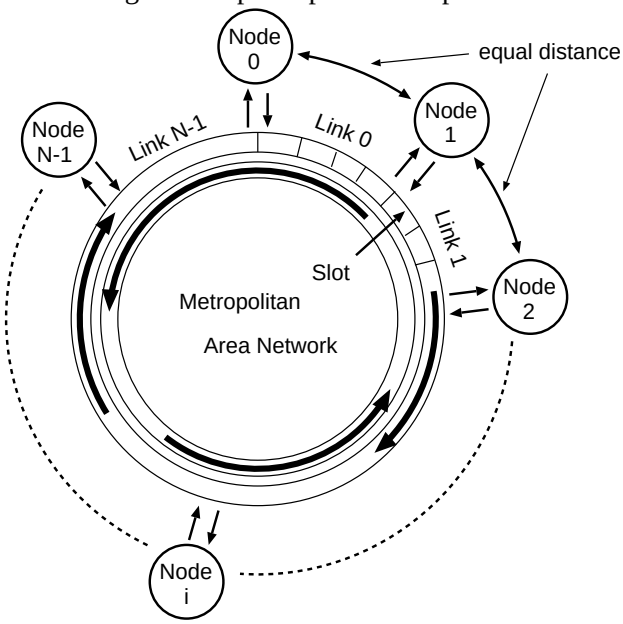


Figure 2: A bidirectional ring with optical compression TDM

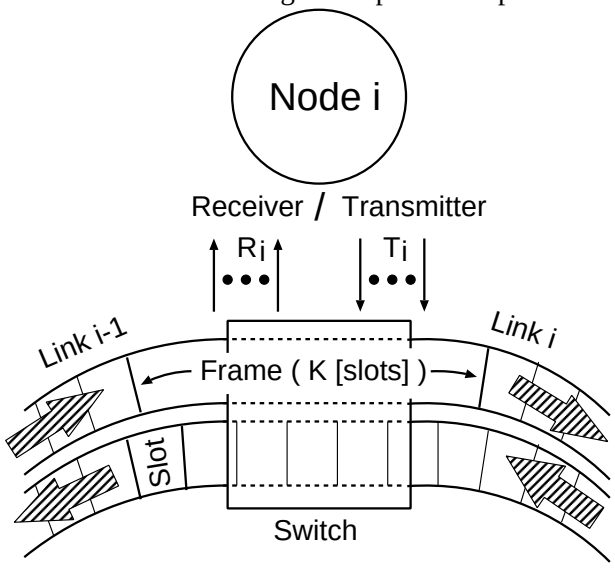


Figure 3: Structure of node $i$

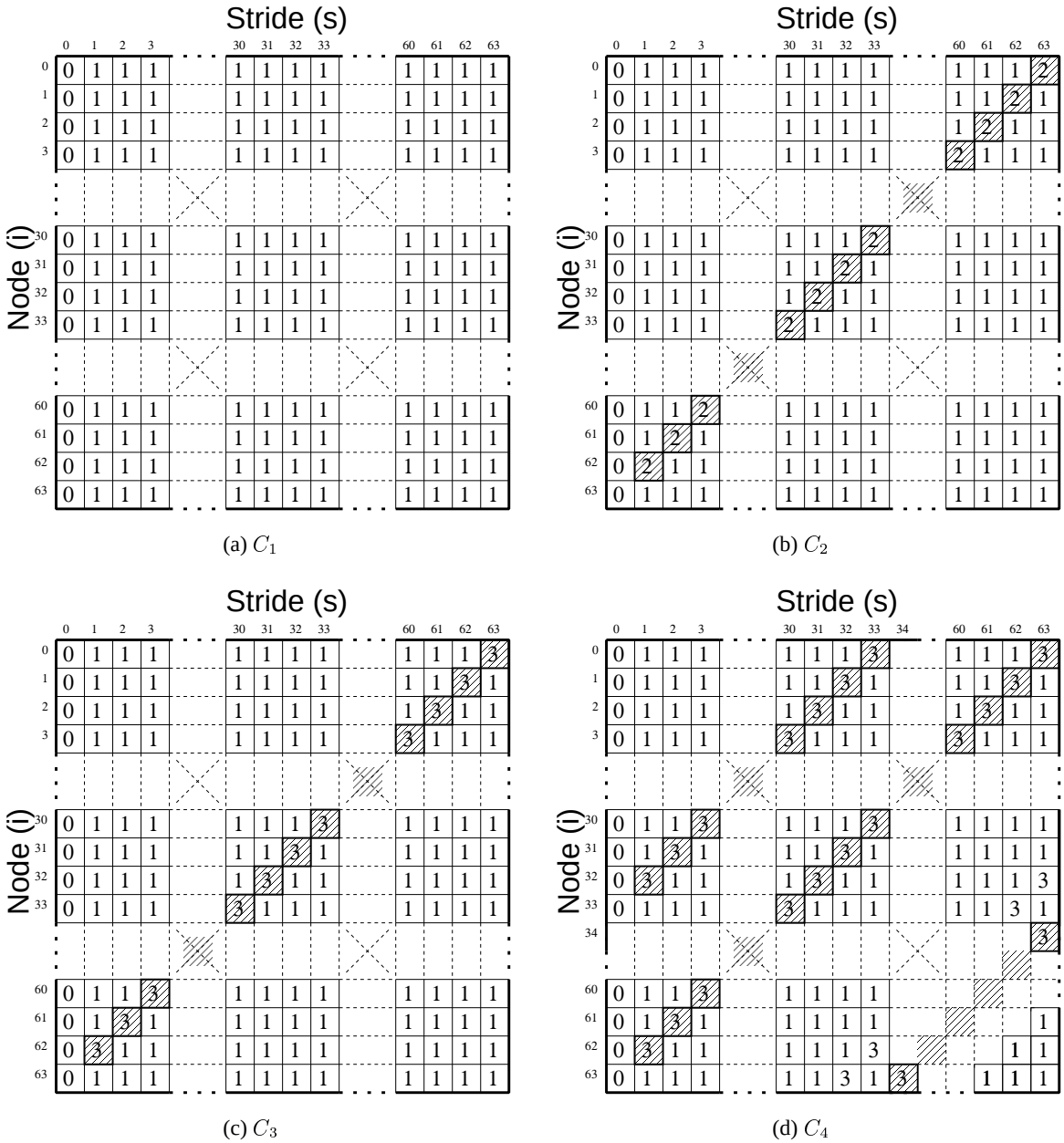


(a) $C_1$

(b) $C_2$

(c) $C_3$

(d) $C_4$

Figure 4: Traffic matrices for numerical examples

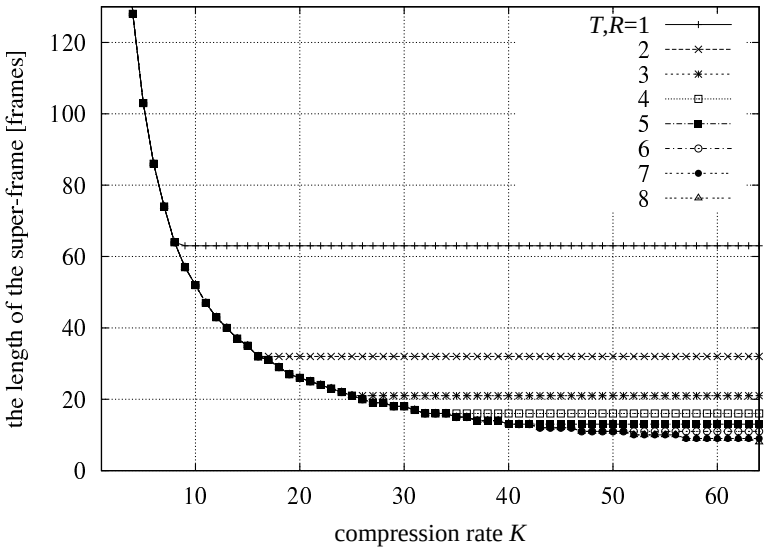


Figure 5: Theoretical lower bounds $LB(64, T, R, K, C_1)$

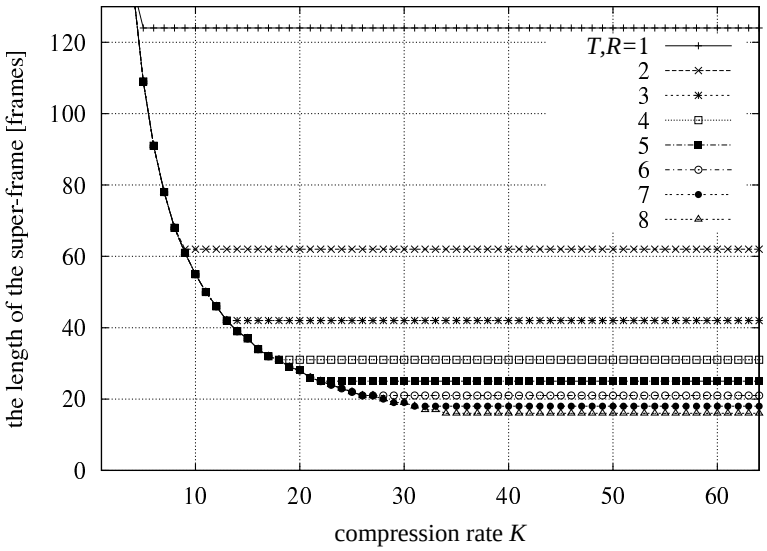


Figure 6: Theoretical lower bounds $LB(64, T, R, K, C_2)$

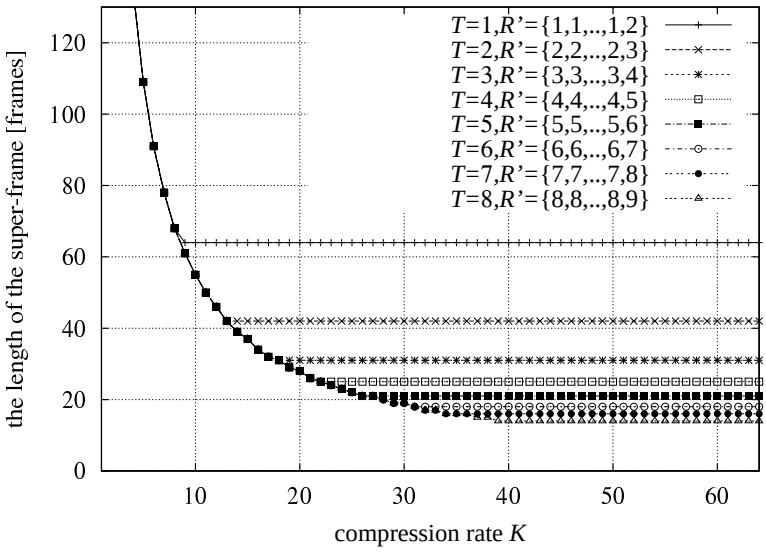


Figure 7: Theoretical lower bounds $LB(64, T, R', K, C_2)$

| | $T=R=1$ | | | | $T=R=2$ | | | |
|---|---|---|---|---|---|---|---|---|
| $K$ | $LB$ | A1 | A2 | A3 | $LB$ | A1 | A2 | A3 |
| 1 | 512 | 527 | 530 | **512** | 512 | 525 | 526 | **512** |
| 2 | 256 | 266 | 267 | **257** | 256 | 264 | 264 | **256** |
| 4 | 128 | 139 | 138 | **129** | 128 | 132 | 132 | **128** |
| 8 | 64 | 85 | 81 | **69** | 64 | 70 | 68 | **64** |
| 16 | 63 | **67** | **67** | 69 | 32 | 43 | 40 | **32** |
| 32 | 63 | 67 | **66** | 69 | 32 | 33 | 33 | **32** |
| 64 | 63 | **63** | **63** | 69 | 32 | **32** | 34 | **32** |
| | $T=R=4$ | | | | $T=R=8$ | | | |
| $K$ | $LB$ | A1 | A2 | A3 | $LB$ | A1 | A2 | A3 |
| 1 | 512 | 525 | 527 | **512** | 512 | 525 | 526 | **512** |
| 2 | 256 | 263 | 265 | **256** | 256 | 263 | 263 | **256** |
| 4 | 128 | 132 | 132 | **128** | 128 | 132 | 132 | **128** |
| 8 | 64 | 66 | 67 | **64** | 64 | 66 | 66 | **64** |
| 16 | 32 | 34 | 34 | **32** | 32 | 33 | 33 | **32** |
| 32 | 16 | 20 | 20 | **16** | 16 | 17 | 17 | **16** |
| 64 | 16 | 17 | 17 | **16** | 8 | 10 | 10 | **8** |

(a) The case of traffic matrix $C_1$

| | $T=R=1$ | | | | $T=R=2$ | | | |
|---|---|---|---|---|---|---|---|---|
| $K$ | $LB$ | A1 | A2 | A3 | $LB$ | A1 | A2 | A3 |
| 1 | 544 | 551 | **546** | 547 | 544 | 545 | **544** | **544** |
| 2 | 272 | 291 | **276** | 285 | 272 | 276 | **273** | **273** |
| 4 | 136 | 170 | 160 | **149** | 136 | 146 | 140 | **138** |
| 8 | 124 | 129 | **126** | 127 | 68 | 86 | 80 | **70** |
| 16 | 124 | **126** | **126** | **126** | 62 | 64 | **63** | 64 |
| 32 | 124 | **126** | **126** | **126** | 62 | **63** | **63** | **63** |
| 64 | 124 | **126** | **126** | **126** | 62 | **63** | **63** | **63** |
| | $T=R=4$ | | | | $T=R=8$ | | | |
| $K$ | $LB$ | A1 | A2 | A3 | $LB$ | A1 | A2 | A3 |
| 1 | 544 | 545 | **544** | **544** | 544 | 545 | 545 | **544** |
| 2 | 272 | **272** | 273 | **272** | 272 | **272** | 273 | **272** |
| 4 | 136 | 138 | 137 | **136** | 136 | 137 | 137 | **136** |
| 8 | 68 | 72 | 70 | **68** | 68 | 69 | 69 | **68** |
| 16 | 34 | 43 | 39 | **35** | 34 | 36 | 35 | **34** |
| 32 | 31 | **32** | **32** | **32** | 17 | 22 | 19 | **18** |
| 64 | 31 | **32** | **32** | **32** | 16 | **16** | **16** | **16** |

(b) The case of traffic matrix $C_2$

| | $T=R=1$ | | | | $T=R=2$ | | | |
|---|---|---|---|---|---|---|---|---|
| $K$ | $LB$ | A1 | A2 | A3 | $LB$ | A1 | A2 | A3 |
| 1 | 576 | 589 | **577** | 581 | 576 | **576** | **576** | **576** |
| 2 | 288 | 322 | **299** | 300 | 288 | 294 | **288** | 289 |
| 4 | 186 | 215 | **192** | 193 | 144 | 162 | 150 | **146** |
| 8 | 186 | 191 | **189** | 190 | 93 | 109 | **97** | **97** |
| 16 | 186 | **189** | **189** | **189** | 93 | 96 | **95** | **95** |
| 32 | 186 | **189** | **189** | **189** | 93 | **95** | **95** | **95** |
| 64 | 186 | **189** | **189** | **189** | 93 | **95** | **95** | **95** |
| | $T=R=4$ | | | | $T=R=8$ | | | |
| $K$ | $LB$ | A1 | A2 | A3 | $LB$ | A1 | A2 | A3 |
| 1 | 576 | **576** | **576** | **576** | 576 | **576** | **576** | **576** |
| 2 | 288 | **288** | **288** | **288** | 288 | **288** | **288** | **288** |
| 4 | 144 | 147 | **145** | **145** | 144 | **144** | **144** | **144** |
| 8 | 72 | 81 | 75 | **73** | 72 | 74 | 73 | **72** |
| 16 | 47 | 54 | **48** | 49 | 36 | 41 | 38 | **37** |
| 32 | 47 | **48** | **48** | **48** | 24 | 27 | **24** | 25 |
| 64 | 47 | **48** | **48** | **48** | 24 | **24** | **24** | **24** |

(c) The case of traffic matrix $C_3$

| | $T=R=1$ | | | | $T=R=2$ | | | |
|---|---|---|---|---|---|---|---|---|
| $K$ | $LB$ | A1 | A2 | A3 | $LB$ | A1 | A2 | A3 |
| 1 | 578 | 594 | **586** | 598 | 578 | **578** | 580 | 590 |
| 2 | 289 | 326 | **309** | 315 | 289 | 298 | **291** | 301 |
| 4 | 186 | 215 | 199 | **194** | 145 | 163 | 155 | **150** |
| 8 | 186 | 191 | **189** | 190 | 93 | 107 | 99 | **97** |
| 16 | 186 | **189** | **189** | **189** | 93 | 96 | **95** | **95** |
| 32 | 186 | **189** | **189** | **189** | 93 | **95** | **95** | **95** |
| 64 | 186 | **189** | **189** | **189** | 93 | **95** | **95** | **95** |
| | $T=R=4$ | | | | $T=R=8$ | | | |
| $K$ | $LB$ | A1 | A2 | A3 | LB | A1 | A2 | A3 |
| 1 | 578 | **578** | 581 | 590 | 578 | **578** | 580 | 590 |
| 2 | 289 | **290** | 291 | 301 | 289 | **290** | 291 | 301 |
| 4 | 145 | 147 | **146** | 148 | 145 | **145** | **145** | 148 |
| 8 | 73 | 80 | 77 | **74** | 73 | 74 | **73** | 74 |
| 16 | 47 | 54 | **49** | **49** | 37 | 41 | 39 | **38** |
| 32 | 47 | **48** | **48** | **48** | 24 | 27 | **24** | 25 |
| 64 | 47 | **48** | **48** | **48** | 24 | **24** | **24** | **24** |

(d) The case of traffic matrix $C_4$

Figure 8: Comparisons of lower bounds and the super-frame lengths obtained by three algorithms

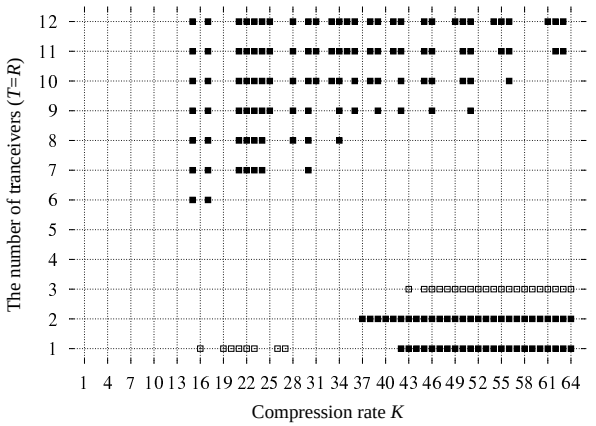


(a) Algorithm A1 for $C_1$

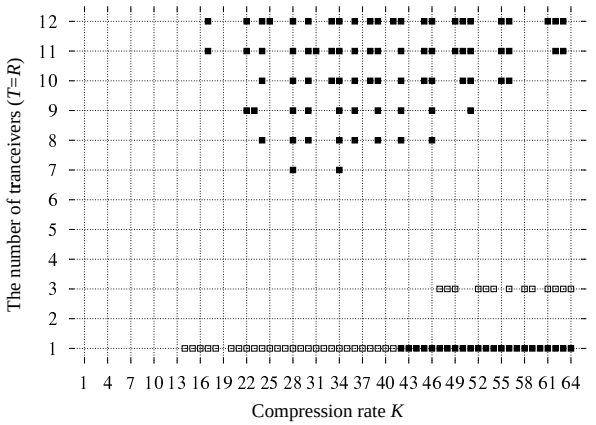


(b) Algorithm A2 for $C_1$

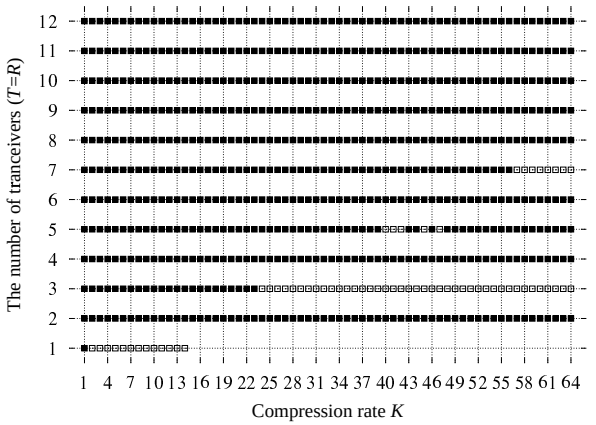


(c) Algorithm A3 for $C_1$

Figure 9: Precise comparisons of results obtained by three algorithms for the traffic matrix $C_1$

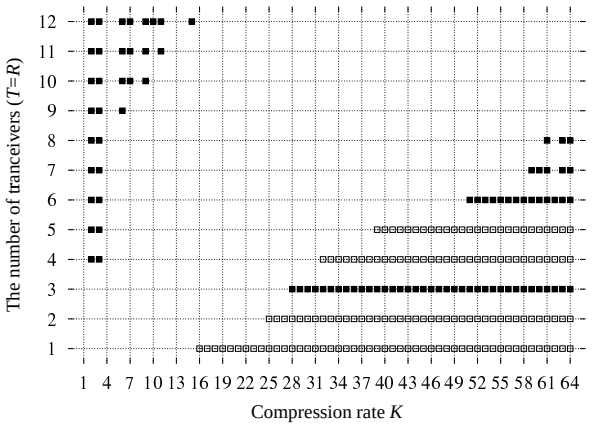


(a) Algorithm A1 for $C_2$

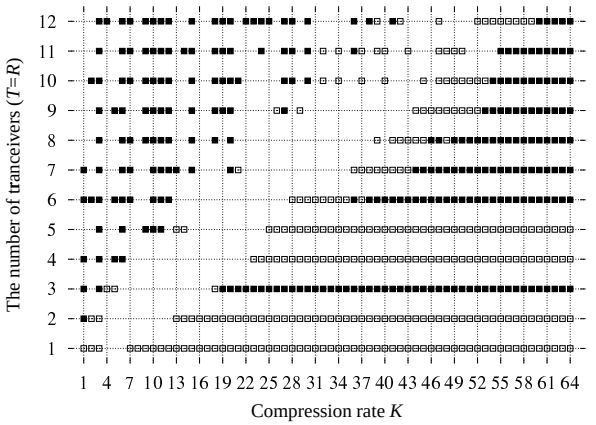


(b) Algorithm A2 for $C_2$

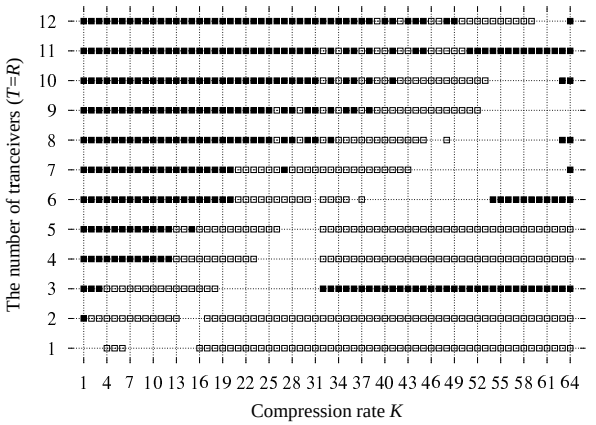


(c) Algorithm A3 for $C_2$

Figure 10: Precise comparisons of results obtained by three algorithms for the traffic matrix $C_2$

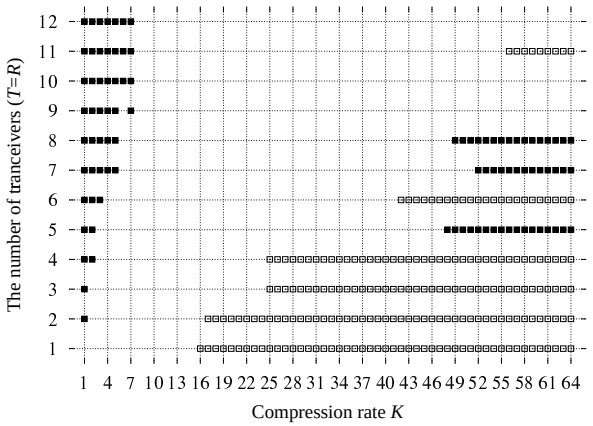


(a) Algorithm A1 for $C_3$

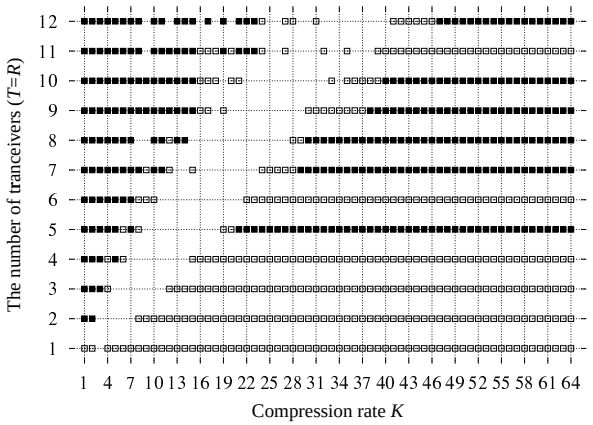


(b) Algorithm A2 for $C_3$

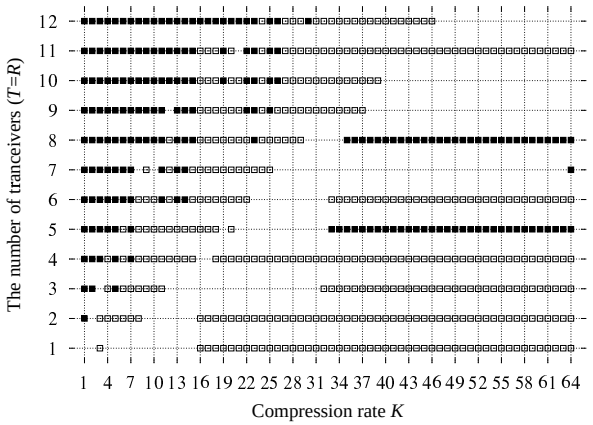


(c) Algorithm A3 for $C_3$

Figure 11: Precise comparisons of results obtained by three algorithms for the traffic matrix $C_3$

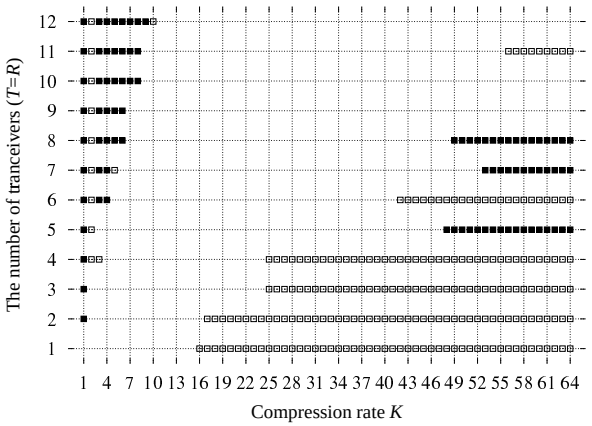


(a) Algorithm A1 for $C_4$

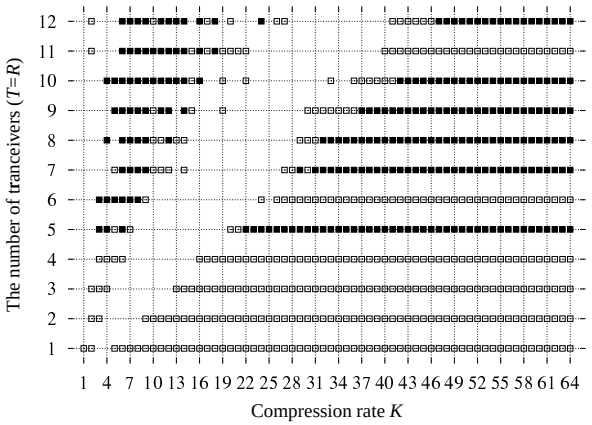


(b) Algorithm A2 for $C_4$

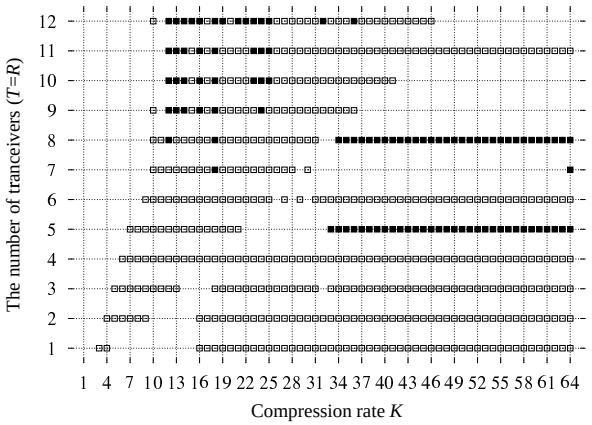


(c) Algorithm A3 for $C_4$

Figure 12: Precise comparisons of results obtained by three algorithms for the traffic matrix $C_4$

Table 1: Parameter Sets for the analysis of the packet delay time.

| Parameter set | A | B | C | D | E | F | G | H | I |
|---|---|---|---|---|---|---|---|---|---|
| Traffic load matrix $C$ | $C_1$ | | | $C_1$ | | | $C_1$ | | |
| The number of transmitters $T$ | 2 | | | 2 | | | 8 | | |
| The number of receivers $R$ | 2 | | | 2 | | | 8 | | |
| Compression rate $K$ | 8 | 16 | 32 | 16 | | | 64 | | |
| The super-frame length $r$ | 64 | 32 | 32 | 43(A1) | 40(A2) | 32(A3) | 8 | | |
| Payload sizes $S_p$ | 53 | | | 53 | | | 53 | 256 | 530 |

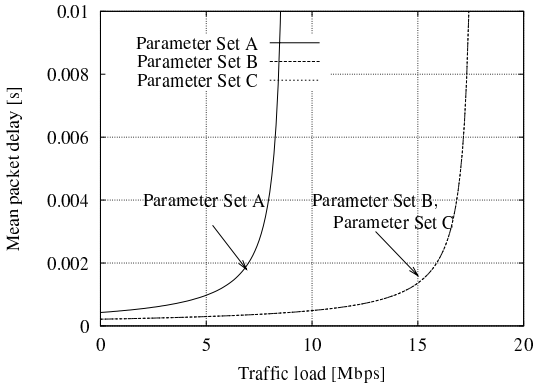


Figure 13: The packet delay times for parameter sets A, B and C

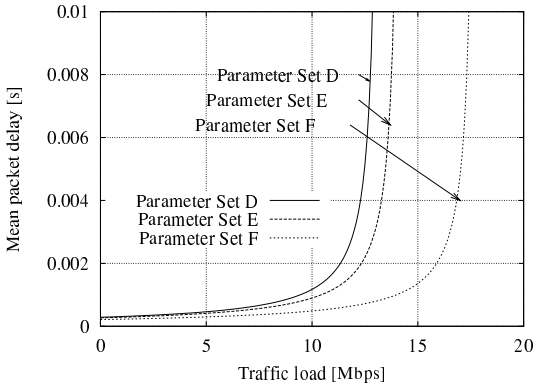


Figure 14: The packet delay times for parameter sets D, E and F

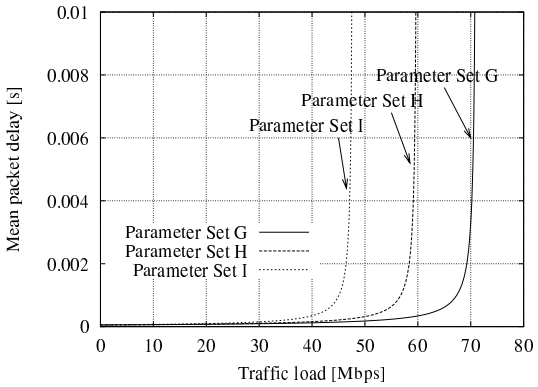


Figure 15: The packet delay time for parameter sets G, H and I